

Thermal divergences of quantum measurement engine

Shanhe Su,^{*} †Zhiyuan Lin,^{*} and Jincan Chen[†]

*Department of Physics, Xiamen University,
Xiamen 361005, People's Republic of China*

Abstract

A quantum engine fueled by quantum measurement is proposed. Under the finite-time adiabatic driving regime, the conversion of heat to work is realized without the compression and expansion of the resonance frequency. The work output, quantum heat, and efficiency are derived, highlighting the important role of the thermal divergence recently reappearing in open quantum systems. The key problem of how the measurement basis can be optimized to enhance the performance is solved by connecting the thermal divergence to the nonequilibrium free energy and entropy. The spin-engine architecture offers a comprehensive platform for future investigations of extracting work from quantum measurement.

^{*}The two authors contributed equally to this work.

[†]Electronic addresses: sushanhe@xmu.edu.cn;jcchen@xmu.edu.cn

1. Introduction

The developments of nuclear magnetic resonance, trapped ions, superconducting circuits, and quantum state tomography facilitate access to the measurement and manipulation of spin ensembles [1, 2]. These techniques have been employed to verify how the laws of thermodynamic emerge in the quantum domain [3, 4]. The existence of the arrow of time in a thermodynamically irreversible process has been demonstrated by observing a fast quenched dynamics of an isolated spin-1/2 system [5]. The reversal of heat flow from a cold spin to a hot spin is possible due to the initial quantum correlation between the spins [6]. An experimental reconstruction of the dynamics of a closed quantum spin showed that the statistical distribution of work satisfies the Tasaki-Crooks theorem and the Jarzynski equality [7]. By integrating the two-point measurement, unitary evolution, and feedback in the control of a spin-1/2 of the ^{13}C nucleus, the fluctuation relation and the non-equilibrium entropy production in the presence of information have been observed [8].

More interestingly, the implementations of quantum machines based on spin systems unlock the potential role of quantum effects in the processes of energy conversion and transport [9–12]. Peterson et al. experimentally implemented a spin engine with an efficiency for work extraction close to Carnot’s efficiency [13]. Assis et al. designed a quantum engine with efficiency higher than the Otto limit, since a reservoir is prepared at a negative effective temperature by inverting the population of a huge nuclear hydrogen spin system [14]. Klatzow and co-workers proved that a coherent superposition enables an engine to produce more power than the equivalent classical counterpart by using an ensemble of nitrogen vacancy centers in diamond as the working substance [15]. Considering the non-Markovian effect, Shirai et al. identified a new definition of work including the energy cost of detaching the spin from the reservoir [16, 17].

A natural question that arises is to unveil the role of quantum measurement in the energy conversion. When quantum measurement collides with spin ensembles, will it be feasible to create the methodology of work extraction in a more flexible and efficient way? It was recently reported that quantum measurement changes the average energy of a quantum system, when the measured observable and the system Hamiltonian do not commute [18–20]. Instead of the stochastic thermal fluctuation from a hot bath, work can be extracted from the stochastic quantum fluctuation induced by the measurement process in quantum Maxwell’s

demon engine [21]. For a two-stroke two-spin device, invasive quantum measurement was regarded as a resource to power the refrigeration [22]. The idea of using the energy provided by the measurement apparatus as the fuel is a fundamental aspect of quantum engines. However, the advantages of adiabatic processes experiencing time-dependent Hamiltonians in quantum measurement engines have not been well revealed. Meanwhile, no simple expressions associated with the heat and work have been obtained so far. The efforts to address these issues will provide general information on how the measurement basis affects the performance of an engine. Thus, the physical implication of the thermal divergence needs to be further excavated because of its simplicity and importance in relating the nonequilibrium free energy and entropy of a quantum state.

In this work, a four-stroke engine, where the quantum measurement and thermalization processes are connected by two thermodynamic adiabatic processes, is built. The quantum measurement process will provide the input energy to ignite the engine. A time-dependent evolution of a spin driven by a rotating magnetic field is applied in the adiabatic processes. Analytical expressions that relate the thermodynamic quantities regarding the thermal divergence, nonequilibrium free energy, and entropy to the heat and work along the cycle will be presented. How the angles of the measurement basis on the Bloch sphere influence the performance will be revealed through the direct relations among the work, efficiency, and the newly defined thermodynamic quantities.

2. The quantum measurement engine

The schematic of the quantum-measurement engine employing a single spin as the working substance is illustrated in Fig. 1. The top and bottom of the loop represent a pair of quasi-parallel and isentropic processes. An isentropic process implies that the von Neumann entropy of the quantum system remains constant in time because of its invariance through unitary evolution, and the system is impermeable to heat during this process. The left and right sides of the loop are a pair of parallel isochoric processes with constant external fields. Heat flows into the cycle through the right quantum measurement process and a part of heat is dumped into the heat sink through the left thermalization process.

The system is in a pseudo-thermal state $\rho_1 = e^{-\beta H_1} / \text{Tr}(e^{-\beta H_1})$ at inverse temperature

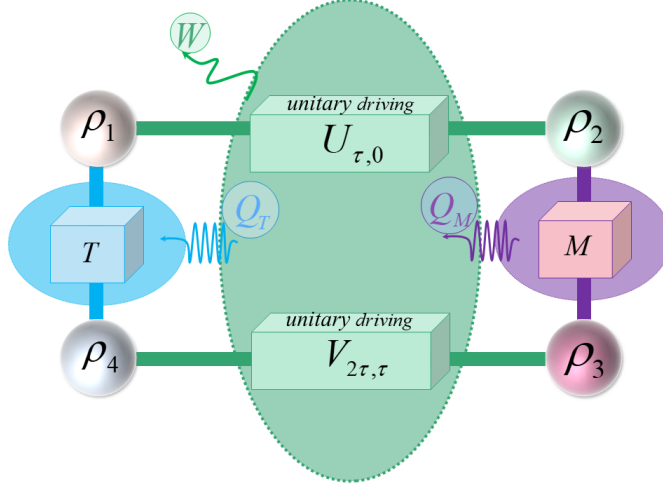


Figure 1: Schematic of the quantum-measurement engine consisting of two adiabatic processes, a quantum measurement process, and a thermalization process.

β and Hamiltonian $H_1 = \frac{\hbar\omega}{2}\sigma_z$, where \hbar is the reduced Planck constant, ω denotes the resonance frequency, and σ_i ($i = x, y, z$) are the Pauli spin operators. During the first stroke (from $t = 0$ to $t = \tau$), the system undergoes a thermally isolated transformation. A time-modulated radiofrequency field resonant with the spin makes Hamiltonian depend on time, which is described by the effective Hamiltonian $H_I(t) = \frac{\hbar\omega}{2}(\cos\frac{\pi t}{2\tau}\sigma_z + \sin\frac{\pi t}{2\tau}\sigma_x)$. At the end of the stroke, the system attains the state $\rho_2 = U_{\tau,0}\rho_1 U_{\tau,0}^\dagger$ with $U_{\tau,0} = \mathcal{T}e^{-\frac{i}{\hbar}\int_0^\tau H_I(t)dt}$ denoting the time-evolution operator and \mathcal{T} being the time-ordering operator, while the Hamiltonian at time $t = \tau$ becomes $H_2 = \frac{\hbar\omega}{2}\sigma_x$. The system consumes an amount of work $W_1 = \text{Tr}(\rho_2 H_2 - \rho_1 H_1)$.

In the second stroke, an instantaneous projective measurement is the testing on the system. For a positive operator-valued measure (POVM) with a set of orthogonal projectors $\{|\chi_1\rangle\langle\chi_1|, |\chi_2\rangle\langle\chi_2|\}$, the post-measurement state ρ_2 is updated to $\rho_3 = \sum_k \pi_k \rho_2 \pi_k$. In this study, we can perform a measurement that projects the spin onto the basis $|\chi_1\rangle = e^{-i\varphi}\sin\frac{\alpha}{2}|\uparrow\rangle - \cos\frac{\alpha}{2}|\downarrow\rangle$ and $|\chi_2\rangle = \cos\frac{\alpha}{2}|\uparrow\rangle + e^{i\varphi}\sin\frac{\alpha}{2}|\downarrow\rangle$. The measurement basis corresponds to measuring the state of the spin in a particular direction. The parameters α and φ are, respectively, interpreted as the colatitude with respect to the z -axis and the longitude with respect to the x -axis in the Bloch sphere representation, where $0 \leq \alpha \leq \pi$ and $0 \leq \varphi < 2\pi$. As the Hamiltonian H_3 of the system corresponding to state ρ_3 remains the same as H_2 , the measurement gives rise to the energy change of the spin $Q_M = \text{Tr}[H_2(\rho_3 - \rho_2)]$,

which will be regarded as the fuel energy of the engine.

During the third stroke (from $t = \tau$ to $t = 2\tau$), the system evolves unitarily according to the Hamiltonian $H_{II}(t) = \frac{\hbar\omega}{2} \left[\cos \frac{\pi(2\tau-t)}{2\tau} \sigma_z + \sin \frac{\pi(2\tau-t)}{2\tau} \sigma_x \right]$, which is a time-reversed protocol of the first adiabatic stroke. The system Hamiltonian is driven from H_3 to H_4 , where H_4 is equivalent to the origin form H_1 of the cycle. The final state of the second adiabatic stroke $\rho_4 = V_{2\tau,\tau} \rho_3 V_{2\tau,\tau}^\dagger$ with the unitary operator $V_{2\tau,\tau} = \mathcal{T} e^{-\frac{i}{\hbar} \int_\tau^{2\tau} H_{II}(t) dt}$. The work performed by the external field is given by $W_2 = \text{Tr}(\rho_4 H_4 - \rho_3 H_3)$. In the last stroke, the system with a time-independent Hamiltonian is coupled to the bath at inverse temperature β . After a sufficiently long time, the system is restored to the initial Gibbs state ρ_1 and releases the heat $Q_T = \text{Tr}[H_1(\rho_1 - \rho_4)]$ to the bath.

3. The roles of the thermal divergence, nonequilibrium free energy, and entropy in the performance

Now, we examine simple expressions for heat and work in thermodynamic processes via establishing the concept of thermal divergence. The quantum Kullback-Leibler-Umegaki divergence (also called relative entropy) [23, 24] is a measure of the entropy of the system at state ρ relative to state σ , given by

$$D(\rho||\sigma) = \text{Tr}[\rho(\ln \rho - \ln \sigma)]. \quad (1)$$

When the reference state σ is a thermal equilibrium state, $D(\rho||\sigma)$ is called the thermal divergence [25]. Thermodynamic quantities, such as heat and work, can be written as functions of thermal divergences of quantum states.

The thermal equilibrium state of a quantum system with Hamiltonians H_i in contact with a heat bath at inverse temperature β is given by the Gibbs state $\sigma_i^{eq} = e^{-\beta H_i} / Z_i$ with the partition function $Z_i = \text{Tr}(e^{-\beta H_i})$. Since $\ln \sigma_i^{eq} = -\beta(H_i - F_i^{eq})$ with $F_i^{eq} = -\beta^{-1} \ln Z_i$ being the Helmholtz free energy, the thermal divergence is then be rewritten as

$$D(\rho_i||\sigma_i^{eq}) = \beta(\mathcal{E}_i - F_i^{eq}) - S_i, \quad (2)$$

where $\mathcal{E}_i = \text{Tr}[H_i \rho_i]$ is the internal energy depending on the expectation value of the system Hamiltonian and $S_i = -\text{Tr}[\rho_i \ln \rho_i]$ is the von Neumann entropy of state i . The thermal divergence has been regarded as a fundamental quantity in quantum thermodynamics because of its connection with the variables of energy and entropy [8, 25]. By introducing the

nonequilibrium free energy [26] of a quantum system as

$$F_i = \mathcal{E}_i - S_i/\beta, \quad (3)$$

the thermal divergence would measure the discrepancy between the nonequilibrium and equilibrium free energies

$$D(\rho_i || \sigma_i^{eq}) = \beta (F_i - F_i^{eq}). \quad (4)$$

In other words, the nonequilibrium free energy of a state is higher than that of the corresponding equilibrium state by an amount equal to the temperature times the thermal divergence.

By using Eq. (2), the net work (Appendix) done on the system in a complete cycle is simplified as

$$\begin{aligned} W &= \frac{1}{\beta} [D(\rho_4 || \sigma_4^{eq}) + D(\rho_2 || \sigma_2^{eq}) - D(\rho_3 || \sigma_3^{eq})] \\ &= F_2 - F_1 + F_4 - F_3. \end{aligned} \quad (5)$$

It is surprised to find that the net work depends only on thermal divergences of quantum states. With the help of Eq. (4), W is simplified into the sum of the changes of the nonequilibrium free energies in the two adiabatic processes. For the second equality, one has considered $S_1 = S_2$ and $S_3 = S_4$ because of the invariant of von Neumann entropy under a unitary evolution, and $F_3^{eq} = F_2^{eq}$ and $F_4^{eq} = F_1^{eq} = F_1$. For extracting energy from the cycle, the net work W are restricted to $W < 0$.

The fuel energy (Appendix) provided by the measurement process is represented by

$$\begin{aligned} Q_M &= \frac{1}{\beta} [D(\rho_3 || \sigma_3^{eq}) - D(\rho_2 || \sigma_2^{eq}) + \Delta S_M] \\ &= F_3 - F_2 + \frac{1}{\beta} \Delta S_M, \end{aligned} \quad (6)$$

where $\Delta S_M = S_3 - S_2$ is the entropy difference of states ρ_3 and ρ_2 and the relation $F_3^{eq} = F_2^{eq}$ has been applied. The fuel energy relies on $D(\rho_3 || \sigma_3^{eq}) - D(\rho_2 || \sigma_2^{eq})$ and ΔS_M . Because the thermalization process interacting with a hot reservoir in a standard Otto cycle has been replaced by a measurement protocol, the input energy Q_M is called as quantum heat. The heat (Appendix) absorbed from the bath in the thermalization process reads

$$\begin{aligned}
Q_T &= \frac{1}{\beta} [-D(\rho_4||\sigma_4^{eq}) + \Delta S_T] \\
&= F_1 - F_4 + \frac{1}{\beta} \Delta S_T,
\end{aligned} \tag{7}$$

where $\Delta S_T = S_1 - S_4$ and the thermal divergence $D(\rho_1||\sigma_1^{eq}) = 0$ have been used. Since the initial and final states are identical in a cycle, the system experiences no change in energy. As a result, $W + Q_M + Q_T = 0$, satisfying the first law of thermodynamics. The thermal efficiency is the net work output divided by the quantum heat provided by quantum measurement

$$\begin{aligned}
\eta &= \frac{-W}{Q_M} \\
&= \frac{D(\rho_3||\sigma_3^{eq}) - D(\rho_4||\sigma_4^{eq}) - D(\rho_2||\sigma_2^{eq})}{D(\rho_3||\sigma_3^{eq}) - D(\rho_2||\sigma_2^{eq}) + \Delta S_M} \\
&= 1 + \frac{F_1 - F_4 - \frac{1}{\beta} \Delta S_M}{F_3 - F_2 + \frac{1}{\beta} \Delta S_M},
\end{aligned} \tag{8}$$

where $\Delta S_T = -\Delta S_M$.

4. The performance of the thermodynamic cycle as an engine

Figs. 2(a) and 2(b) show the contour plots of the work output $-W$ and efficiency η versus the colatitude α and longitude φ , parameterized in $\hbar\omega = 0.5\text{peV}$, $\tau = 8.4\mu\text{s}$, and $\beta = 1/\hbar\omega_0$. Quantum measurements act as a powerful tool for manipulating quantum states and providing the fuel energy to drive the engine. Interestingly, the performance of the cycle can be enhanced by optimizing the direction of the measurement basis. The contour plots exhibit two qualitatively different regimes separated by $\varphi = \pi$. For $0 \leq \varphi \leq \pi$, $-W$ shows maxima at $\alpha_W = 1.10$ and $\varphi_W = 1.77$, while η achieves the peak at $\alpha_\eta = 1.15$ and $\varphi_\eta = 2.04$. In the range of $\pi \leq \varphi \leq 2\pi$, the distributions of $-W$ and η as functions of α and φ satisfy antisymmetry with respect to the axis $\alpha = \pi/2$ and translational invariance, i.e., $-W(\alpha, \varphi) = -W(\pi - \alpha, \varphi + \pi)$ and $\eta(\alpha, \varphi) = \eta(\pi - \alpha, \varphi + \pi)$.

A thermal divergence $D(\rho_i||\sigma_i^{eq})$ relates the internal energy \mathcal{E}_i , the free energy F_i^{eq} , and von Neumann entropy S_i . The thermal divergence also measures the difference between the

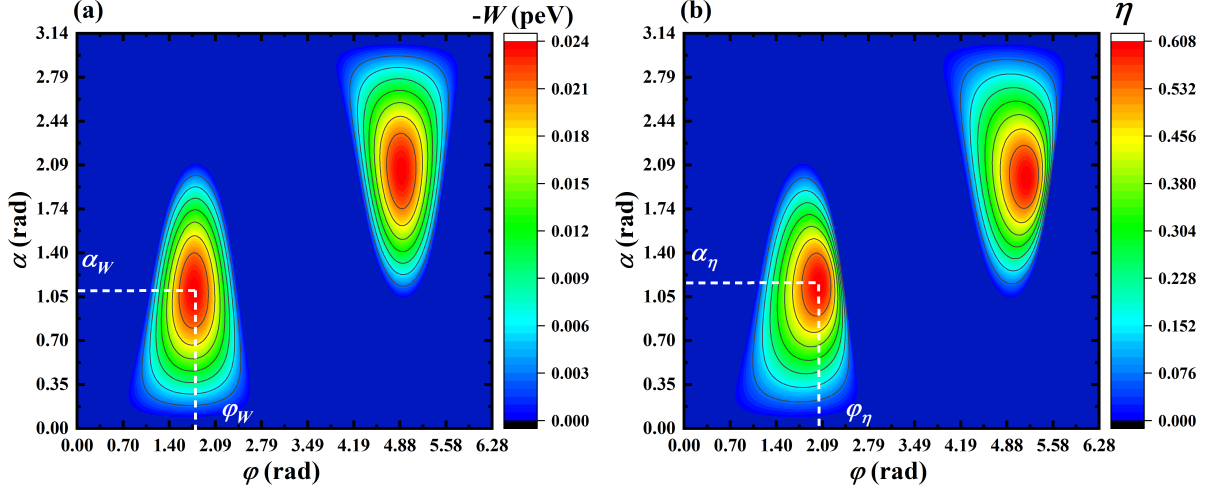


Figure 2: (a) The work output $-W$ and (b) the efficiency η varying with the colatitude α and longitude φ .

nonequilibrium free energy F_i and equilibrium free energy F_i^{eq} . To quantify the advantage of using the concept of the thermal divergence, we first plot $-W$, Q_M , and η [the thermal divergences $D(\rho_3||\sigma_3^{eq})$ and $D(\rho_4||\sigma_4^{eq})$, entropy difference ΔS_M , and nonequilibrium free energies F_3 and F_4] as functions of the colatitude α , as shown in Fig. 3(a) [Fig. 3(b)]. Note that the curves of $D(\rho_2||\sigma_2^{eq})$, F_1 , and F_2 are not displayed in Fig. 3(b), because they are constant values at a given time of the adiabatic process.

Based on numerical simulations, we observe that $-W$ increases as φ increases in the range of $\alpha \leq \alpha_{W'}$. The reason can be attributed to the enhancement of the difference $D(\rho_3||\sigma_3^{eq}) - D(\rho_4||\sigma_4^{eq})$ of thermal divergences. For $\alpha \geq \alpha_{W'}$, the difference $D(\rho_3||\sigma_3^{eq}) - D(\rho_4||\sigma_4^{eq})$ tends to decrease, yielding low $-W$ again. From the second equality in Eq. (5) and Fig. 3(b), changing the difference of thermal divergences is in fact modifying the discrepancy of nonequilibrium free energies $F_3 - F_4$, which is a part of the energy available to perform thermodynamic work. The quantum heat Q_M is closely linked to the changes of the nonequilibrium free energy F_3 and the entropy difference ΔS_M due to the measurement process [Eq. (6)]. However, F_3 and ΔS_M in the range between $\varphi_{W'}$ and φ_η are relatively small, such that the cycle use fewer inputs Q_M to produce more output $-W$. Figs. 3(c) and (d) show how the work output and the efficiency are improved by adjusting the longitude φ . $-W$ has a maximum value at $\varphi = \varphi_{W'}$, which is condition for the largest values of the differences $D(\rho_3||\sigma_3^{eq}) - D(\rho_4||\sigma_4^{eq})$ and $F_3 - F_4$ as well. After reaching the maximum

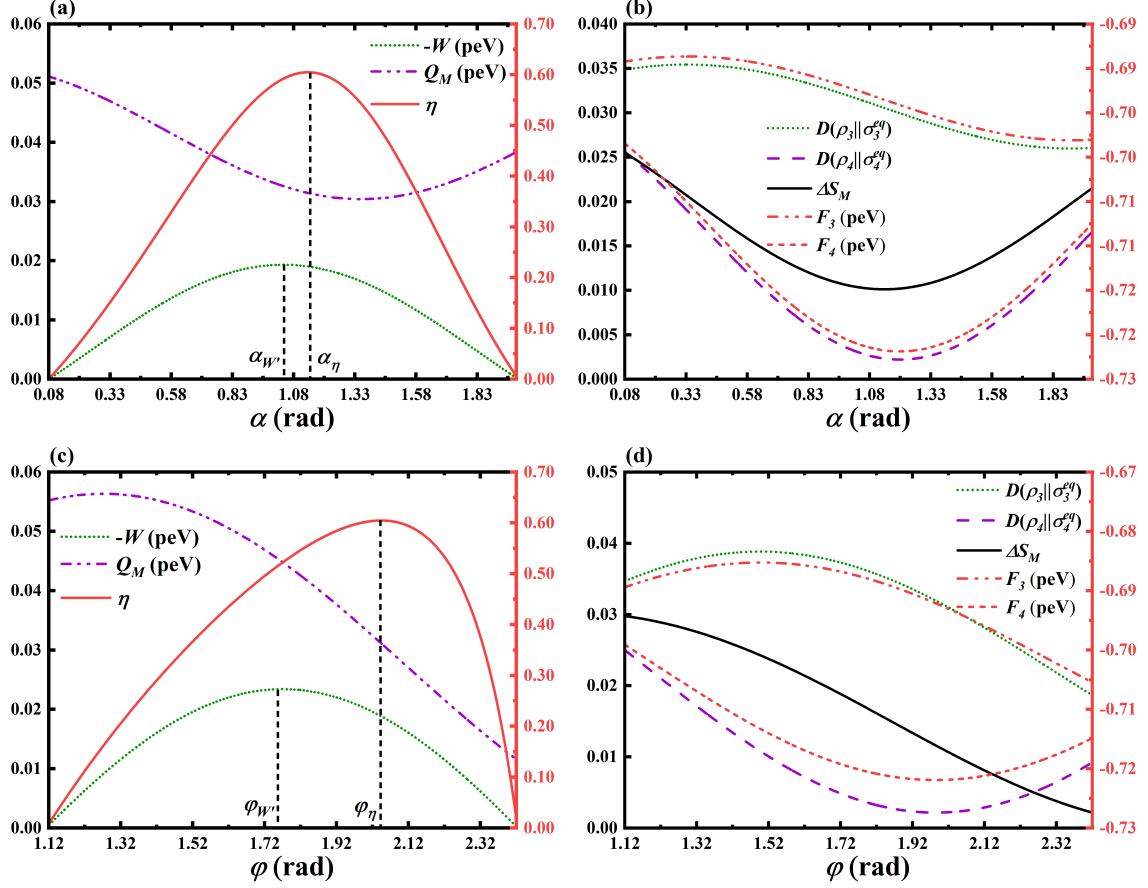


Figure 3: For a given value φ_η of φ , the curves of (a) the work output $-W$, quantum heat Q_M , and efficiency η and (b) the thermal divergences $D(\rho_3||\sigma_3^{eq})$ and $D(\rho_4||\sigma_4^{eq})$, entropy difference ΔS_M , and nonequilibrium free energies F_3 and F_4 varying with the colatitude α . For a given value α_η of α , the curves of (c) the work output $-W$, input energy Q_M , and efficiency η and (d) the thermal divergences $D(\rho_3||\sigma_3^{eq})$ and $D(\rho_4||\sigma_4^{eq})$, entropy difference ΔS_M , and nonequilibrium free energies F_3 and F_4 varying with longitude φ . In (a) and (c), the left vertical axis shows values for $-W$ and Q_M , while the corresponding scale of η is on the right vertical axis. In (b) and (d), the left vertical axis shows values for $D(\rho_3||\sigma_3^{eq})$, $D(\rho_4||\sigma_4^{eq})$, and ΔS_M , while the corresponding scales of F_3 and F_4 are on the right vertical axis.

work output, $D(\rho_3||\sigma_3^{eq})$, F_3 , and ΔS_M are reduced with the growth of φ , leading to a rapid decrease in Q_M . Therefore, the maximum efficiency is obtained at the point φ_η larger than φ_W . Overall, one can efficiently generate work from quantum engine by optimizing the parameters with respect to the measurement basis.

5. Conclusions

In this paper, a measurement based spin engine has been developed to show how quantum measurement is able to fuel an engine. By considering finite-time adiabatic driven operations, the compression and expansion of the spin transition frequency during the adiabatic stages are not necessary for the work extraction. Analytical expressions of heat and work are derived, highlighting the role of the thermal divergence. We employed the relationship among the thermal divergence, nonequilibrium free energy, and energy entropy to find how the measurement basis can be optimized to improve the work output and the efficiency. The results obtained here will encourage new experimental efforts to explore engines driven by quantum measurement.

Acknowledgments

This work has been supported by the National Natural Science Foundation of China(Grant No. 11805159 and 12075197) and the Natural Science Foundation of Fujian Province (No. 2019J05003).

APPENDIX: THE HEAT AND WORK OF EACH PROCESS

1. Process I—First adiabatic process

The system is initially in thermal equilibrium with the thermal divergence $D(\rho_1||\sigma_1^{eq}) = 0$, and its internal energy is related to the free energy and the entropy of state ρ_1 as

$$\mathcal{E}_1 = \frac{1}{\beta} S_1 + F_1 = \frac{1}{\beta} S_1 + F_1^{eq}. \quad (9)$$

According to Eq.(2), the internal energy of the system after the unitary evolution from $t = 0$ to $t = \tau$ is given by

$$\mathcal{E}_2 = \frac{1}{\beta} [D(\rho_2||\sigma_2^{eq}) + S_2] + F_2^{eq}. \quad (10)$$

The equality $S_1 = S_2$ holds because of the fact that the von Neumann entropy is invariant with respect to a unitary transformation. Since the system is not connected to the heat

bath during process I, the work W_1 done by external field is expected to be the change of the internal energy of the system, i.e.,

$$\begin{aligned} W_I &= \mathcal{E}_2 - \mathcal{E}_1 \\ &= \frac{1}{\beta} D(\rho_2 || \sigma_2^{eq}) + F_2^{eq} - F_1^{eq}. \end{aligned} \quad (11)$$

2. Process II—Quantum measurement

The quantum measurement process converts the system into state ρ_3 with the internal energy

$$\mathcal{E}_3 = \frac{1}{\beta} [D(\rho_3 || \sigma_3^{eq}) + S_3] + F_3^{eq}. \quad (12)$$

The instantaneous projective measurement does change the Hamiltonian of the system, resulting in the free energy difference $F_3^{eq} - F_2^{eq} = 0$. Consequently, the change of the internal energy of the working substance caused by Q_M during quantum measurement is straightforward given by

$$\begin{aligned} Q_M &= \mathcal{E}_3 - \mathcal{E}_2 \\ &= \frac{1}{\beta} [D(\rho_3 || \sigma_3^{eq}) - D(\rho_2 || \sigma_2^{eq}) + S_3 - S_2], \end{aligned} \quad (13)$$

which can be regarded as the fuel energy for the quantum engine.

3. Process III—Second adiabatic process

In the second adiabatic process, the system experiences a time-dependent unitary evolution until reaching the internal energy

$$\mathcal{E}_4 = \frac{1}{\beta} [D(\rho_4 || \sigma_4^{eq}) + S_4] + F_4^{eq}. \quad (14)$$

Similarly, the von Neumann entropy of the system remains constant throughout process III, such that $S_4 = S_3$. The work performed on the system becomes

$$\begin{aligned}
W_{III} &= \mathcal{E}_4 - \mathcal{E}_3 \\
&= \frac{1}{\beta} [D(\rho_4 || \sigma_4^{eq}) - D(\rho_3 || \sigma_3^{eq})] + F_4^{eq} - F_3^{eq}.
\end{aligned} \tag{15}$$

With the help of Eqs. (11) and (15), the total average work W done on the system is the sum of W_I and W_{III}

$$\begin{aligned}
W &= W_I + W_{III} \\
&= \frac{1}{\beta} [D(\rho_4 || \sigma_4^{eq}) + D(\rho_2 || \sigma_2^{eq}) - D(\rho_3 || \sigma_3^{eq})],
\end{aligned} \tag{16}$$

where the relations $F_3^{eq} = F_2^{eq}$ and $F_4^{eq} = F_1^{eq} = F_1$ have been applied.

4. Process IV—Thermalization

When the system is put into contact with the thermal bath, the full thermalization process drives the system back to the initial state ρ_1 . The energy change of the system is caused by the heat Q_T flowing from the heat bath, i.e.,

$$\begin{aligned}
Q_T &= \mathcal{E}_1 - \mathcal{E}_4 \\
&= \frac{1}{\beta} [-D(\rho_4 || \sigma_4^{eq}) + S_1 - S_4].
\end{aligned} \tag{17}$$

-
- [1] E. A. Chekhovich, S. F. C. da Silva, A. Rastelli, Nuclear spin quantum register in an optically active semiconductor quantum dot, *Nat. Nanotechnol.* 15, 999-1004 (2020).
- [2] M. Jiang, T. Wu, J. W. Blanchard, G. Feng, X. Peng, and D. Budker, Experimental benchmarking of quantum control in zero-field nuclear magnetic resonance, *Sci. Adv.* 4, eaar6327 (2018).

- [3] R. Uzdin and S. Rahav, Global passivity in microscopic thermodynamics, *Phys. Rev. X* 8, 021064 (2018).
- [4] S. Pal, S. Saryal, D. Segal, T. S. Mahesh, and B. K. Agarwalla, Experimental study of the thermodynamic uncertainty relation, *Phys. Rev. Research* 2, 022044(R) (2020).
- [5] T. B. Batalhão, A. M. Souza, R. S. Sarthour, I. S. Oliveira, M. Paternostro, E. Lutz, and R. M. Serra, Irreversibility and the arrow of time in a quenched quantum system, *Phys. Rev. Lett.* 115, 190601 (2015).
- [6] K. Micadei, J. P. S. Peterson, A. M. Souza, R. S. Sarthour, I. S. Oliveira, G. T. Landi, T. B. Batalhão, R. M. Serra, and E. Lutz, Reversing the direction of heat flow using quantum correlations, *Nat. Commun.* 10, 2456 (2019).
- [7] T. B. Batalhão, A. M. Souza, L. Mazzola, R. Auccaise, R. S. Sarthour, I. S. Oliveira, J. Goold, G. De Chiara, M. Paternostro, and R. M. Serra, Experimental reconstruction of work distribution and study of fluctuation relations in a closed quantum system, *Phys. Rev. Lett.* 113, 140601 (2014)
- [8] P. A. Camati, J. P. S. Peterson, T. B. Batalhão, K. Micadei, A. M. Souza, R. S. Sarthour, I. S. Oliveira, and R. M. Serra, Experimental rectification of entropy production by Maxwell's demon in a quantum system, *Phys. Rev. Lett.* 117, 240502 (2016).
- [9] H. T. Quan, Y. Liu, C. P. Sun, and F. Nori, Quantum thermodynamic cycles and quantum heat engines, *Phys. Rev. E* 76, 031105 (2007).
- [10] Y. Hong, Y. Xiao, J. He, and J. Wang, Quantum Otto engine working with interacting spin systems: Finite power performance in stochastic thermodynamics, *Phys. Rev. E* 102, 022143 (2020).
- [11] C. Ou, Y. Yokoi, S. Abe, Spin isoenergetic process and the Lindblad equation, *Entropy* 21,

- 503 (2019).
- [12] S. Su, X. Luo, J. Chen, and C. Sun, Angle-dependent quantum Otto heat engine based on coherent dipole-dipole coupling, *Europhys. Lett.* 115, 30002 (2016).
- [13] J. P. S. Peterson, T. B. Batalhão, M. Herrera, A. M. Souza, R. S. Sarthour, I. S. Oliveira, and R. M. Serra, Experimental characterization of a spin quantum heat engine, *Phys. Rev. Lett.* 123, 240601 (2019).
- [14] R. J. de Assis, T. M. de Mendonça, C. J. Villas-Boas, A. M. de Souza, R. S. Sarthour, I. S. Oliveira, and N. G. de Almeida, Efficiency of a quantum otto heat engine operating under a reservoir at effective negative temperatures, *Phys. Rev. Lett.* 122, 240602 (2019).
- [15] J. Klatzow, J. N. Becker, P. M. Ledingham, C. Weinzetl, K. T. Kaczmarek, D. J. Saunders, J. Nunn, I. A. Walmsley, R. Uzdin, and E. Poem, Experimental demonstration of quantum effects in the operation of microscopic heat engines, *Phys. Rev. Lett.* 122, 110601 (2019).
- [16] Y. Shirai, K. Hashimoto, R. Tezuka, C. Uchiyama, and N. Hatano, Non-Markovian effect on quantum Otto engine: Role of system-reservoir interaction, *Phys. Rev. Research* 3, 023078 (2021).
- [17] G. Guarnieri, C. Uchiyama, and B. Vacchini, Energy backflow and non-Markovian dynamics, *Phys. Rev. A* 93, 012118 (2016).
- [18] K. Brandner, M. Bauer, M. T. Schmid, and U. Seifert, Coherence-enhanced efficiency of feedback-driven quantum engines, *New J. Phys.* 17, 065006 (2015).
- [19] C. Elouard, D. A. Herrera-Martí, M. Clusel, and A. Auffèves, The role of quantum measurement in stochastic thermodynamics, *npj Quantum Inf.* 3, 9 (2017).
- [20] J. Yi, P. Talkner, and Y. W. Kim, Single-temperature quantum engine without feedback

- control, *Phys. Rev. E* 96, 022108 (2017).
- [21] C. Elouard, D. Herrera-Martí, B. Huard, and A. Auffèves, Extracting work from quantum measurement in Maxwell's Demon engines, *Phys. Rev. Lett.* 118, 260603 (2017).
- [22] L. Buffoni, A. Solfanelli, P. Verrucchi, A. Cuccoli, and M. Campisi, Quantum measurement cooling, *Phys. Rev. Lett.* 122, 070603 (2019).
- [23] H. Spohn, Entropy production for quantum dynamical semigroups, *J. Math. Phys.* 19, 1227-1230 (1978).
- [24] G. Manzano, F. Galve, R. Zambrini, and J. M. R. Parrondo, Entropy production and thermodynamic power of the squeezed thermal reservoir, *Phys. Rev. E* 93, 052120 (2016).
- [25] P. A. Camati, J. F. G. Santos, and R. M. Serra, Coherence effects in the performance of the quantum Otto heat engine, *Phys. Rev. A* 99, 062103 (2019).
- [26] M. Esposito and C. Van den Broeck, Second law and Landauer principle far from equilibrium, *Europhys. Lett.* 95, 40004 (2011).